Hindawi
Journal of Engineering
Volume 2023, Article ID 1481943, 13 pages
https://doi.org/10.1155/2023/1481943

Research Article

An Evaluation Method of Ship-Tracking Algorithms for High-Frequency Surface Wave Radar considering High Maneuvers Generated by the MMG Model

Iswandi, Risanuri Hidayat, and Sigit B. Wibowo

Department of Electrical Engineering and Information Technology, Faculty of Engineering, Universitas Gadjah Mada, Yogyakarta 55281, Indonesia

Correspondence should be addressed to Iswandi; iswandi@ugm.ac.id

Received 16 March 2022; Revised 11 April 2023; Accepted 2 May 2023; Published 15 May 2023

Academic Editor: Kamran Iqbal

Thelong-distance coverage of high-frequency surface wave radar (HFSWR) has promoted it as an enormous means for ship monitoring on the country's maritime territory. Since it is a primaryradar, noncooperative targets can also be detected. However, this radar also has a shortcoming of low spatial and temporal resolutions due to the narrow available bandwidth in the HF band. This limitation can reduce the performance of ship detection and tracking, especially for highly maneuvering ships. This paper proposes a new method to assess the tracking algorithm for a high-maneuvering ship. The absence of a high-maneuvering plot in the AIS data and existing analytical models are replaced by the MMG model run on MANSIM software. The linear, turning, and zigzag motions are generated and used to evaluate the tracking algorithms. The Monte Carlo simulation was conducted regarding the degradation of spatial resolution in the higher radial range. The tracking performance was analyzed by calculating the RMSE of four parameters, i.e., absolute position, radial range, bearing angle, and speed. For a trial case, four tracking algorithms were evaluated, i.e., Kalman filter (KF), extended Kalman filter (EKF), unscented Kalman filter (UKF), and particle filter (PF). The evaluation results showed that the EKF tracker had a minor error for the linear track with RMSE of absolute position, radial range, bearing angle, and speed being 1.368 km, 0.526 km, 1.550°, and 0.005 m/s, respectively. Otherwise, the UKF performed slightly better than EKF for the high maneuver targets. The RMSE of absolute position, radial range, bearing angle, and speed were 1.649 km, 0.639 km, 1.919°, and 0.165 m/s, respectively. The results also ensure the applicability of the MMG model to evaluate the tracking algorithm's performance in HFSWR.

1. Introduction

The HFSWR is an effective maritime remote sensor covering a long distance of 200 nmi and has various functions, including ship detection and tracking. As a primary radar, it can provide continuous and real-time monitoring. Beneficially, it can detect noncooperative ships, which turns off the automatic identification system (AIS) radio. Thus, it can fill in the shortcoming of AIS [1].

Beyond the advantages of HFSWR for monitoring ships, it has some challenges in the detection and tracking process. The Bragg components produced by the interaction between dynamic sea waves and radar signals cause a high false alarm for ship detection [2]. Besides, the ionospheric clutter and radio frequency interference can mask the scattering signal of the ships [3]. Another challenge in developing ship detection on HFSWR is the low spatial resolution of radar detection, including the radial range and the azimuth resolution [4]. The relatively narrow bandwidth on the HF band produces a radial range resolution that is much larger than the ship dimension. Moreover, the azimuth resolution in the radial coverage area causes a lower resolution at a farther distance from the radar location, which produces a higher deviation of the detected ship location.

Although the sailing ships are statistically moving in regular linear track and low maneuver, those with illegal mission sail with ghost mode or turn off the AIS transmitter and make a high maneuver to hide from the radar monitor.

In addition, the military vessel is also possible to do so. Therefore, the tracking of high-maneuvering ships is necessary to be investigated. Unfortunately, the low resolution of HF radar detection affects the performance of the ship tracking processes. The maneuver or sudden change of ship motion can degrade the tracking accuracy [5]. Therefore, a more robust tracking algorithm is required to track high maneuvers, which is still a challenging problem in ship detection by HFSWR.

Generally, the tracking algorithm in the research is verified by two kinds of data. Firstly, the empirical data gathered by AIS are utilized as the tracking reference [5]. The sailing ship is mandatorily equipped with an AIS transmitter which regularly broadcasts its information, including position and velocity. The AIS receiver collects the signal and the data, which can be used to assess the tracking results of HF radars. However, the linear tracks dominate the data for any assessment of the tracking algorithm [6, 7]. The AIS data are sometimes suffered from track fragmentation which can reduce the availability of ground truth data for this study [8]. Wang et al. proposed a grammar-based model based on AIS data mining representing the ship maneuver scenario to assess the tracking algorithm performance [9]. Of course, the considered ship maneuvers are limited by the existing scheme in the dataset and possibly missing some other possible plots. Furthermore, Wang's work is more concerned with evaluating the algorithm's ability to track multiple ships simultaneously. Secondly, the theoretical tracks produced by a specific mathematical model are used to test the performance of the tracking algorithm [10]. An effort to include ship maneuvers has been proposed by Zhang et al. with the assumption of constant velocity and constant turn of ship motion [11]. The theoretical data are more controllable and provide a more exact ship position but a less natural characteristic of ship maneuvers. The effect of ship maneuvers is also discussed in terms of data integrity on AIS systems regarding the multitrack detection.

Meanwhile, ship maneuverability in naval architecture and ocean engineering is commonly expressed by mathematical models categorized into the whole ship and modular models [12]. The whole-ship model constructs a maneuver from the total hydrodynamic forces and moments acting upon a complete entity of the vessel. In comparison, the modular model considers the hydrodynamic forces working on separate modules of ship elements, such as hull, rudder, and propeller, to produce ship maneuvers. A famous modular model has been proposed by a research group called the maneuvering modeling group (MMG) at the Japanese towing tank conference (JTTC) as named as MMG model [13]. The MMG model calculates the ship maneuver based on the hydrodynamic force on the different modules, i.e., hull, rudder, and propeller. The model's ability to simulate various possible ship motions can be adopted to assess the tracking algorithm performance in HFSWR. To the best of the authors' knowledge, this idea has not been presented in any literature before. Thus, it becomes the main contribution of this paper.

Our research proposed evaluating the tracking algorithm by considering the ship's high maneuvers generated with the MMG model HFSWR. This paper uses an MMG model-based software, i.e., MANSIM [14], to generate the ship tracks. The validity of MANSIM in the empirical measurement of full-scale or miniaturized ships has been reported [15]. Next, the maneuver model is combined with the HFSWR signal model in our previous work [16]. The detection results of combined two radar stations are computed and used for input of tracking systems. The performance of four tracking algorithms, i.e., Kalman filter (KF), extended Kalman filter (EKF), unscented Kalman filter (UKF), and particle filter (PF), are evaluated on three ship maneuvers: linear, turning, and zigzag. Since the radar coverage is radial basis, the radar resolution is gradually decreasing in the farther distance. The Monte Carlo simulation is conducted to randomize the initial ship position and heading to handle this issue. Finally, the tracking performance is evaluated by calculating the root mean square error (RMSE) of absolute position, radial range, bearing angle, and speed [4].

The rest of the paper is organized as follows. Section 2 describes the research method that consists of the tracking algorithm and evaluation method. Section 3 reports the results of model implementation on the defined scenario and the evaluation of tracking algorithms. Finally, Section 4 summarizes the research findings and future works.

2. Research Methods

This paper aims to evaluate the performance of the tracking algorithm considering the effect of ship maneuvers. Subsequently, the MANSIM software was taken into account to generate the ship tracks based on the MMG model and fed as the input to the HFSWR simulator. The sequential data of ship detection were used to evaluate the performance of the tracking algorithms. Figure 1 shows the block diagram of the research method for tracking performance evaluation.

Initially, the MMG model generated linear, turning, and zigzag maneuvers. Then, the Monte Carlo simulation was brought into account to randomize the initial position and heading of the ships. The tracks were inputted to the two independent HFSWRs, i.e., Radar A and Radar B. Four popular algorithms were assessed in the current works: KF, EKF, UKF, and PF. The performance of those trackers was observed by calculating the RMSE of the detected tracks compared to the exact positions in rectangular and spherical coordinate systems.

Figure 2 describes the developed ship tracking system and data generation with the MMG model. The tracking algorithm functions to estimate the ship's trajectory ($\mathbf{x}_k$) from the sequence of the ship's position ($\mathbf{z}_n$), as shown in the end process in Figure 2. The input to this system is in the radar received signal, fed to the receiving antenna elements, which form the receiving array. The receiving array consists of n-element antennas where each n^{th} antenna element receives the radar receiver signal scattered by the ship ($\mathbf{S}_{r,n}$). The signal received by all elements of the receiving array is processed by a series of processes to detect the target position sequence (z_n). The details of signal processing and detection methods are not discussed here but can be found in our previous publication [16].

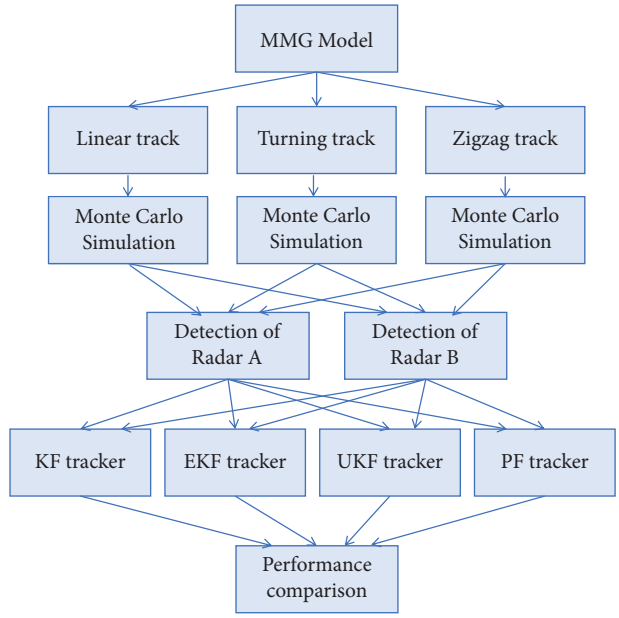

Figure 1: Block diagram of the proposed method to evaluate the performance of tracking algorithms on the maneuvering ship tracks generated by the MMG model.

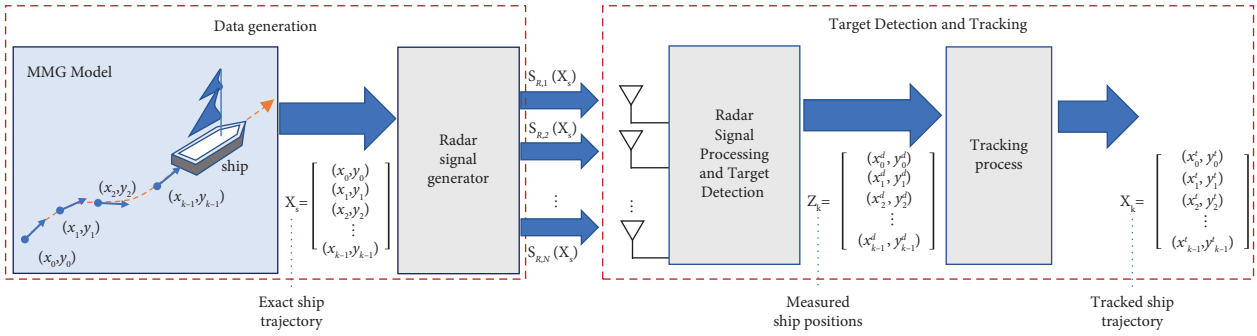

Figure 2: Data flow from MANSIM to simulator in the current evaluation.

The considered radar is the FMCW radar; so the radar reception signal is a copy of the broadcast signal with attenuation and time delay. The attenuation and the time delay are calculated from the radar receiving antenna and the scattering target positions. In this case, the target is referred to as the ship. In the current model, the MMG model generates the ship position, as shown by the left block of Figure 2. In this data generation process, the MMG model generates ship track data which consists of successive points in the coordinate system from (x_0, y_0) to (x_{k-1}, y_{k-1}), where k is the number of data samples. This track data are then stored in the form of vector $\mathbf{x}_s$. The ship's position sequence on the trajectory made with the MMG model is then used to calculate the radar-received signal sequence. So, the input for the ship tracking system is HF RADAR signal data from the reflection of a moving ship with the trajectory obtained from the MMG model.

The last process is for testing the ability of the radar tracking algorithm. The radar target detection system produces a series of ship positions ($\mathbf{z}_k$) used as input for the tracking algorithm being tested. The accuracy of the tracking algorithm is measured by comparing the track results ($\mathbf{x}_k$) with the actual path ($\mathbf{x}_s$) generated by the MMG model.

2.1. Radar Specification. In this paper, the HFSWR configuration is considered in this work's prior publication [16]. The radar is monostatic with a frequency modulated continuous wave (FMCW) waveform and a linear array type antenna on the receiver. The radar configuration is listed in Table 1, which is chosen for proper ship detection following the work of Dzvonkovskaya et al. [17].

A single radar covered an area of 120° azimuthal wide, and the maximum range was set to 80 km. The 1.5 km radar range resolution was obtained from the 100 kHz bandwidth based on the relation of $c/2B$, where B is radar signal bandwidth (Hz) and $c = 3{\cdot}10^8$ m/s is the radio wave speed in free space. The radar deployed 16 elements of an array antenna to provide the azimuth resolution approximated to 7.5° by assuming the beamwidth of uniform linear array (ULA) [18].

Table 1: Radar specification in the simulation.

Radar parameters	Descriptions
Center frequency	10 MHz
Waveform	FMCW
Chirp repetition frequency	2 Hz
Transmitted power	0 dBW
Bandwidth (B)	100 kHz
Inter-radar spacing	40 km
Tx antenna	Dipole
Rx antenna	16-element array
Gain of Tx antenna and Rx array element	2.15 dBi
Interelement spacing of Rx array	$\lambda/2$
Range resolution	1.5 km
Maximum range	80 km
Azimuth resolution	7.5°
Azimuth coverage	120°
Coherent integration times	256 s
Overlapped Doppler map	75%
Time resolution of detection	32 s
Speed resolution	0.1172 m/s
Maximum speed detection	15 m/s

The 2 Hz chirp repetition frequency with 28 sampling per chirp provided the CIT of 128 s. The radar could detect the target with the maximum absolute speed of 15 m/s or 29.16 knots in this configuration. Following the reference work, the target detection had a 75% overlapped Doppler map. Thus, it could provide position updates every 32 s [13]. In addition, two identical radars were assumed in the simulation scene with a 40 km separation and an 18° slanted angle to obtain the maximum overlapped area. The predefined position and direction radars are shown in Figure 3 to indicate the radar coverage area.

There were two coordinate systems used to represent the position in space and moving ship. The space coordinate system of space was annotated by x_0-y_0-z_0 with o_0 as the origin point. The x_0-y_0 plane coincided with the water surface, and the z_0 axis was vertically downward. The moving ship position was presented by x-y-z, with the origin point o was located in the midship. The x-axis was directed to the bow of the ship.

The other parameters are also drawn in Figure 4. The total ship velocity is represented by $U = \sqrt{u^2 + v_m^2}$, where u and v_m are velocity components along x and y axes. The ship's center of gravity is assumed in the midship position and located in (x_G, 0, 0) in the x-y-z system. The lateral velocity in the center of gravity is defined by the following equation:

$$v = v_m + x_G r, \tag{1}$$

where r is yaw rate and x_G is the ship's center of gravity. The ship motion consists of three components: yaw, sway, and surge. Those components relate to the hydrodynamic forces with the following relationships [13]:

$$\begin{aligned} m(\dot{u} - vr) &= X, \\ m(\dot{v} + ur) &= Y, \\ I_{zG}\dot{r} &= N_m, \end{aligned} \tag{2}$$

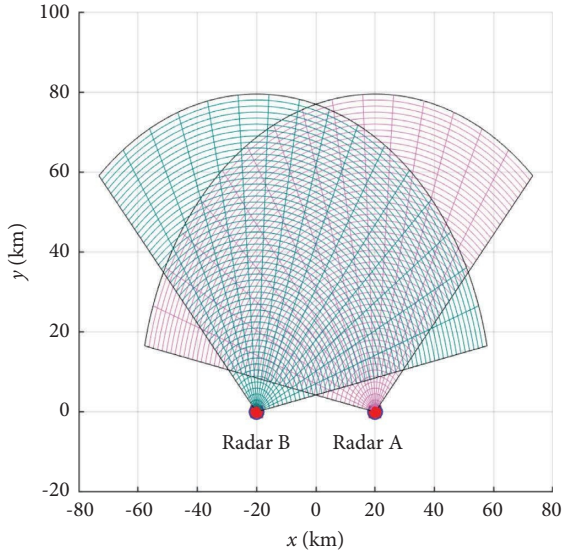

Figure 3: The radars' position in the coordinate system and their overlapped coverage area.

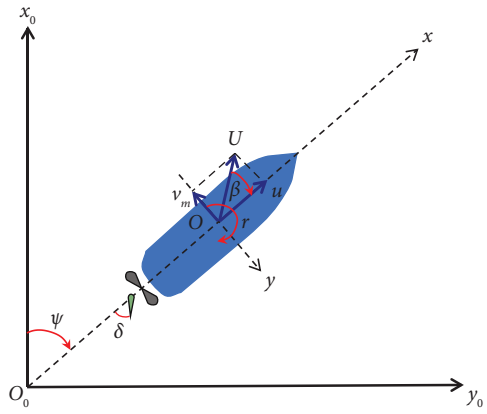

Figure 4: Coordinate system on the MMG model.

where I_{zG} is the moment inertia of a ship around the center of gravity. The dot notation in $\dot{u}, \dot{v}$, and $\dot{r}$ means the first-time derivation. X, Y, and N_m are the hydrodynamic forces and moments acting on the center of gravity, further derived from the modular components.

$$\begin{aligned} X &= X_H + X_R + X_P, \\ Y &= Y_H + Y_R, \\ N_m &= N_H + N_R. \end{aligned} \tag{3}$$

The subscripts H, R, and P mean hull, rudder, and propeller, respectively. All parameters on the right-hand side of (3) are the components of hydrodynamic forces that act on the ship. Those components are derived based on many parameters from the simulated ships. The complete expression of each parameter can be found in [13].

In this paper, the ship track was generated by using the MMG model run on a software named MANSIM [14]. This software has been validated to the empirical measurements on the full scale or miniaturized ships [15].

Figure 5 shows the interface of MANSIM, which contains a sort of predefined parameters to simulate the ship maneuvers by the MMG model and the resulting track. The current work used the KVLCC2 tanker in the reference published by Yasukawa and Yoshimura [13]. The tanker's principal specification is listed in Table 2 to provide a glance at the ship. Besides the parameters listed in Table 2, some hydrodynamic coefficients were also needed during the simulation. This paper does not mention those parameters, but they are provided in [13].

The MMG model is elaborated in this paper to simulate three basic maneuvers: linear, turning, and zigzag with the driving parameters listed in Table 3. Those motions are simulated by assuming the constant propeller revolution, which produces the initial speed of 10 m/s. The motion is generated by the rudder angle set to 35°. The zigzag maneuver is simulated with the steering pattern 10/10 (10 s of +35° and 10 s of −35°, alternately).

2.2. Tracking Algorithms. Various tracking algorithms have been known in the radar fields. However, the HFSWR has a unique challenge due to its low spatial and temporal resolutions, high-density multitarget, and being interfered with by sea clutter. Various tracking algorithms have been proposed to work on the HFSWR that can be categorized based on the linearity of the target motion model. Based on the presumption that most of the vessels move on linear trajectories, some linear algorithms have been proposed for HF radar, such as the alpha-beta (AB) tracker [19] and Kalman filter (KF) tracker [5, 20, 21]. The KF tracker was the improved version of the AB tracker to be more adaptive to the target maneuvers.

However, the ship sometimes moves in nonlinear motion during the maneuver, which reduces the accuracy of linear trackers. Therefore, there are some modifications of the KF tracker to work on nonlinear motion, such as extended Kalman filter (EKF) [22, 23], unscented Kalman filter (UKF) [23], and particle filter (PF) [24]. In this paper, the performance of those nonlinear trackers was evaluated on the turning and zigzag tracks. In addition, the KF filter was also included as a comparison.

The explanation of those trackers is started from the target dynamic model from the state of two-dimensional moving targets with nearly constant velocity expressed in general matrix form as follows [25]:

$$\mathbf{x}_k = \mathbf{f}\left(\mathbf{x}_{k-1}, \mathbf{u}k\right) + \mathbf{w}_k, \tag{4}$$

where $\mathbf{f}(\cdot)$ is the dynamic model function, $\mathbf{x}_k$ is the target state vector in the time k containing position, $\mathbf{w}_k$ is the Gaussian noise of the process, and $\mathbf{u}_k$ is the control vector. Next, the radar measurement as the input of tracking can be expressed by the following equation:

$$\mathbf{z}_k = \mathbf{H}\left(\mathbf{x}_\mathbf{k}\right) + \mathbf{v}_k, \tag{5}$$

where $\mathbf{z}_k$ is radar measurement data in the time k, $\mathbf{H}(\cdot)$ is the measurement model function, and $\mathbf{v}_k$ is the measurement noise.

The tracking process consisted of four steps: prediction, innovation, correction, and updating, which can be briefly described as follows.

2.2.1. Prediction. The position is predicted at time k based on target state on time k-1

$$\widetilde{\mathbf{x}}_k = \mathbf{f}\left(\mathbf{x}_{k-1}, \mathbf{u}_k\right), \tag{6}$$

where the tilde means the predicted value. The Kalman filter uses the linear motion model, so equation (6) can be derived as follows:

$$\widetilde{\mathbf{x}}_k = \mathbf{F}_{k-1}\widetilde{\mathbf{x}}_{k-1}, \tag{7}$$

where the transition matrix $\mathbf{F}_k$ is defined as

$$\mathbf{F}_k = \begin{bmatrix} 1 & T_k & 0 & 0 \\ 0 & 1 & 0 & 0 \\ 0 & 0 & 1 & T_k \\ 0 & 0 & 0 & 1 \end{bmatrix}, \tag{8}$$

where T_k is the radar time resolution.

The other algorithm uses nonlinear motion models. For example, the Taylor series expansion for the EKF is

$$\mathbf{f}\left(\widetilde{\mathbf{x}}_k\right) = \mathbf{f}\left(\widetilde{\mathbf{x}}_{k-1}, \mathbf{u}_\mathbf{k}\right) + \mathbf{J}\left(\widetilde{\mathbf{x}}_{k-1}\right)\left(\mathbf{x}_{k-1} - \widetilde{\mathbf{x}}_{k-1}\right), \tag{9}$$

where $\mathbf{J}()$ is the Jacobian function. The prediction step also estimates the following predicted covariance:

$$\mathbf{P}_k = \mathbf{F}_k\mathbf{P}_{k-1}\mathbf{F}_k^T + \mathbf{Q}_k, \tag{10}$$

where $\mathbf{F}_k$ is the Jacobian of the state and $\mathbf{Q}_k$ is the process noise covariance matrix.

2.2.2. Innovation. New information is gathered from the measurement on time k for calculating the measurement residual and formulating the innovation matrix $\mathbf{S}_k$. The measurement of residual and innovation matrix for the Kalman filter is calculated by the following equation:

$$\begin{aligned} \mathbf{y}_k &= \mathbf{z}_k - \mathbf{H}\widetilde{\mathbf{x}}_k, \\ \mathbf{S}_k &= \mathbf{K}_k\left(\mathbf{z}_k - \mathbf{H}\widetilde{\mathbf{x}}_k\right), \end{aligned} \tag{11}$$

where $\mathbf{H}$ is the transition matrix and $\mathbf{K}_k$ is the weight equation or commonly called the Kalman gain. For the EKF, this process was calculated by the following equation:

$$\begin{aligned} \mathbf{y}_k &= \mathbf{z}_k - \mathbf{H}\left(\widetilde{\mathbf{x}}_k\right), \\ \mathbf{S}_k &= \mathbf{H}_k\mathbf{P}_{k-1}\mathbf{H}_k^T + \mathbf{R}_k, \end{aligned} \tag{12}$$

where $\mathbf{R}_k$ is the covariance matrix of measurement noise and $\mathbf{H}_k$ is the jacobian of the state.

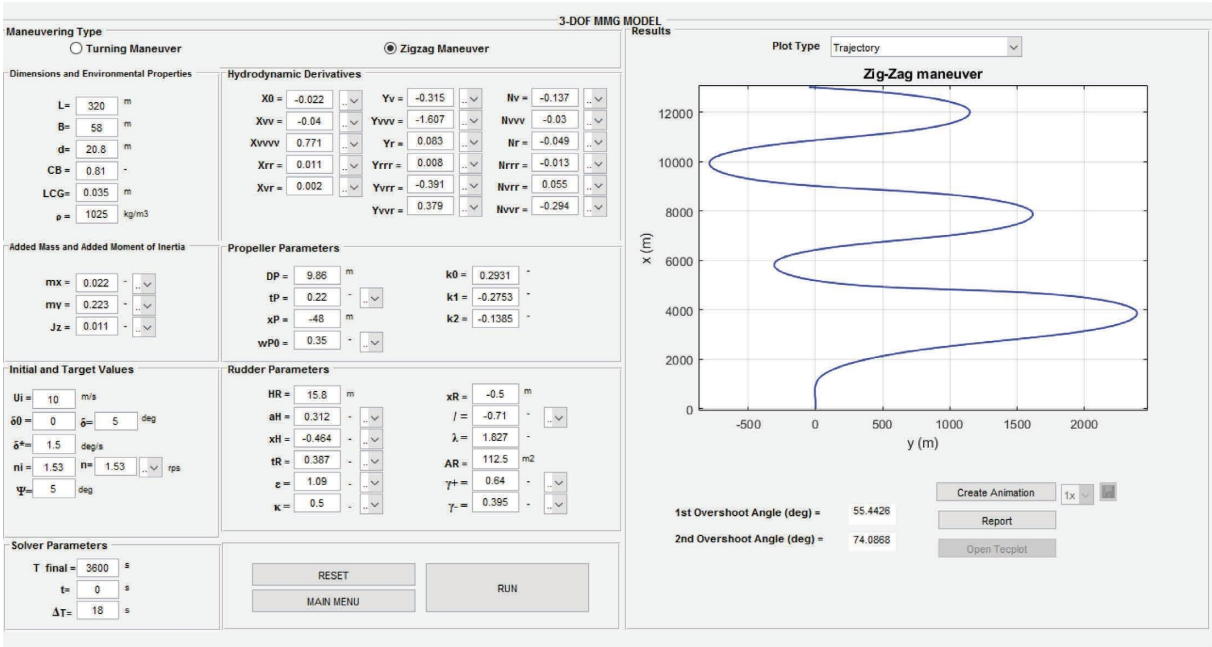

Figure 5: The example of MANSIM interface to simulate the zigzag track based on the MMG model.

Table 2: Specification of the KVLCC2 ship in the simulation [13].

Ships parameters	Value
Ship length between perpendicular (L_{pp})	320 m
Ship breadth	58 m
Ship draft	20.8 m
Displacement volume of ship	312.6 m^3
Effective inflow angle to the rudder	11.2 m
Block coefficient	0.810
Propeller diameter	9.86 m
Rudder span length	15.8 m
Profile area of a movable part of a marine rudder	112.5 m^2

Table 3: Parameters for the ship maneuvers.

Parameters	Value
Initial speed (m/s)	10
Rudder angle	35°
Rudder steering rate (°/s)	1.76
Radius of yaw gyration	$0.25L_{pp}$
Steering pattern	10/10

2.2.3. Correction. The target state is estimated with the correction from the innovation. This process generally can be expressed as

$$\hat{\mathbf{x}}_k = \mathbf{F}_k\tilde{\mathbf{x}}_k + \mathbf{S}_k. \tag{13}$$

The hat was used to sign the predicted value. In addition, the covariance matrix was also corrected by using the innovation data:

$$\hat{\mathbf{P}}_k = \mathbf{P}_k - K_k\mathbf{S}_k\mathbf{K}_k^T, \tag{14}$$

2.2.4. Updation. Information is updated for the next iteration.

The difference between the methods is on how to calculate the Kalman gain and assumed dynamic model function. The detailed explanation of the tracking algorithm is not explained in this paper and can be found in [26].

2.3. Method of Performance Evaluation. This paper aims to assess the tracking performance in three maneuvers with the following scenarios:

(1) Linear track: 10 m/s constant speed and 60 minutes durations.

(2) Turning maneuver: since the turning duration was relatively short, it used mixed of 20 minutes linear, 20 minutes turning, and 20 minutes linear tracks with 10 m/s speed. The turning angle varied from 35°.

(3) Zigzag maneuver: it had a 60 minutes duration and 10 m/s speeds, while the turning angle was also set from 35°.

Note that the radar detection gave the update position every 32 s. Therefore, radar detection provided 112 updates along the 60 minutes of considering track durations.

The radar coverage area in Figure 3 is a radial shape. Consequently, the patch in the further range is more extensive than the closer one. It means that the radar resolution varies with the radial distance. Each maneuver was randomly spread in the radar coverage to handle this variation by taking into account the Monte Carlo (MC) simulation as done in the work of Zhang et al. [11].

The MC simulation generated random initial positions and the heading of the ship. The initial position was set $-40 < x_0 < 40$ km and $10 < y_0 < 70$ km, while the heading was from 0 to 360° to keep the track inside the radar coverage.

Next, the tracking performance was evaluated by comparing the tracking results to the exact ship position and velocity. The error measurements were quantized into the following four parameters:

(i) The RMSE of absolute position in Cartesian coordinate [27] was calculated by the Euclidean distance between the tracking result to the exact track.

$$p_{rmse} = \sqrt{\frac{1}{N_k}\sum_{k=1}^{N_k}\left[\left(x_k' - x_k\right)^2 + \left(y_k' - y_k\right)^2\right]}, \quad (15)$$

where x and y are the coordinates in the Cartesian coordinate with the prime symbol referring to the tracking results. While N_k is the number of the time step.

(ii) The RMSE of the radial range is the distance relative to the origin point between two radar stations [8].

$$\rho_{rmse} = \sqrt{\frac{1}{N_k}\sum_{k=1}^{N_k}\left[\left(\rho_k' - \rho_k\right)^2\right]}, \quad (16)$$

where ρ is the radial distance relative to the origin point.

$$\rho = \sqrt{x^2 + y^2}. \quad (17)$$

(iii) The RMSE of the bearing angle or the bearing of the target position is relative to the radar look direction.

$$\theta_{rmse} = \sqrt{\frac{1}{N_k}\sum_{k=1}^{N_k}\left[\left(\theta_k' - \theta_k\right)^2\right]}, \quad (18)$$

where

$$\theta = \operatorname{atan}\frac{y}{x}. \quad (19)$$

(iv) The RMSE of speed or the nondirectional velocity was defined by the following equation:

$$v_{rmse} = \sqrt{\frac{1}{N_k}\sum_{k=1}^{N_k}\left[\left(v_{x,k}^{'} - v_{x,k}\right)^2 + \left(y_{y,k}^{'} - y_{y,k}\right)^2\right]}, \quad (20)$$

where $v_{x,k}$ and $v_{y,k}$ are the target velocity at k time step and in the x and y axis direction, respectively.

3. Results and Discussion

This paper presents the utilization of the MMG model to test the ship tracking algorithm in HFSWR. The model can provide many realistic and modifiable maneuvers to input on the radar simulator and further tracking assessments. Basically, the MMG model can create various ship movements; however, the turning and zigzag motions are chosen to be presented in this paper.

3.1. The Spatial Resolution of Radar Detection. As previously discussed, the limited bandwidth available for HFSWR causes low spatial and temporal resolutions. A radar detection test was initially tested to show the effect of those limitations. A ship with linear motion was randomly placed on the radar scene, as shown in Figure 6(a). Two radar stations were taken into account to make the comparison. As shown in Figure 6(a), both radars observe the linear target motion as a nonlinear track due to the low spatial and temporal resolutions. To show the detection error, the differences in radial range, bearing angle, and radial speed were calculated and shown in Figures 6(b)–6(d), respectively. The quantitative errors are listed in Table 4. The average radial range error is 0.4625 km. This error makes sense because the radar range resolution is 1.5 km, as shown in Table 1. Likewise, the bearing angle error of 2.217° is acceptable for the angle resolution of 7.5°. The average error of radial speed is 0.121 m/s, which looked slightly higher than the speed resolution of 0.1172 m/s, but it still confirms the absolute target speed of 10 m/s.

It should be noted that radar signal detection uses different mechanisms. The target range is measured from the receiving time delay, influenced by the sampling frequency. In contrast, the speed is acquired from the Doppler frequency shift, controlled by the coherence integration time instead of the radar spatial resolution. Therefore, the result of speed detection in Figure 6(d) has a smoother graph compared to range measurement in Figures 6(a)–6(c).

The comparison of the detection error of radar A and B, as listed in Table 4, shows that radar A has a higher error. It can be observed that the distance between the target location and radar A is farther than radar B. The detection error is gradually increasing for the farther distance since the detection is conducted radially. In this research, the effect of the error gap due to distance is compensated by generating multiple measurements with the target location spread in the radar scene.

3.2. The Maneuvering Ship Tracks Generated by MANSIM. Figure 7(a) shows the result of the turning maneuver based on the MMG model and generated by MANSIM. All turning tests were conducted with 20 s duration and 1 s time resolution. The configuration set the ship to complete a full turning with the duration was kept constant. The rudder was varied from 10° to 35°, while the propeller rotation speed was kept constant to give constant absolute velocity. The figure shows that the higher rudder angle gives a smaller turning radius. Since 35° is the maximum rudder angle in regular ship operation, this maneuver basically gives the smallest turning radius of the ship under test. It is worth noticing that the turning radius in any turning maneuver is not constant. It differs from the result of those modeled by a simple circle equation.

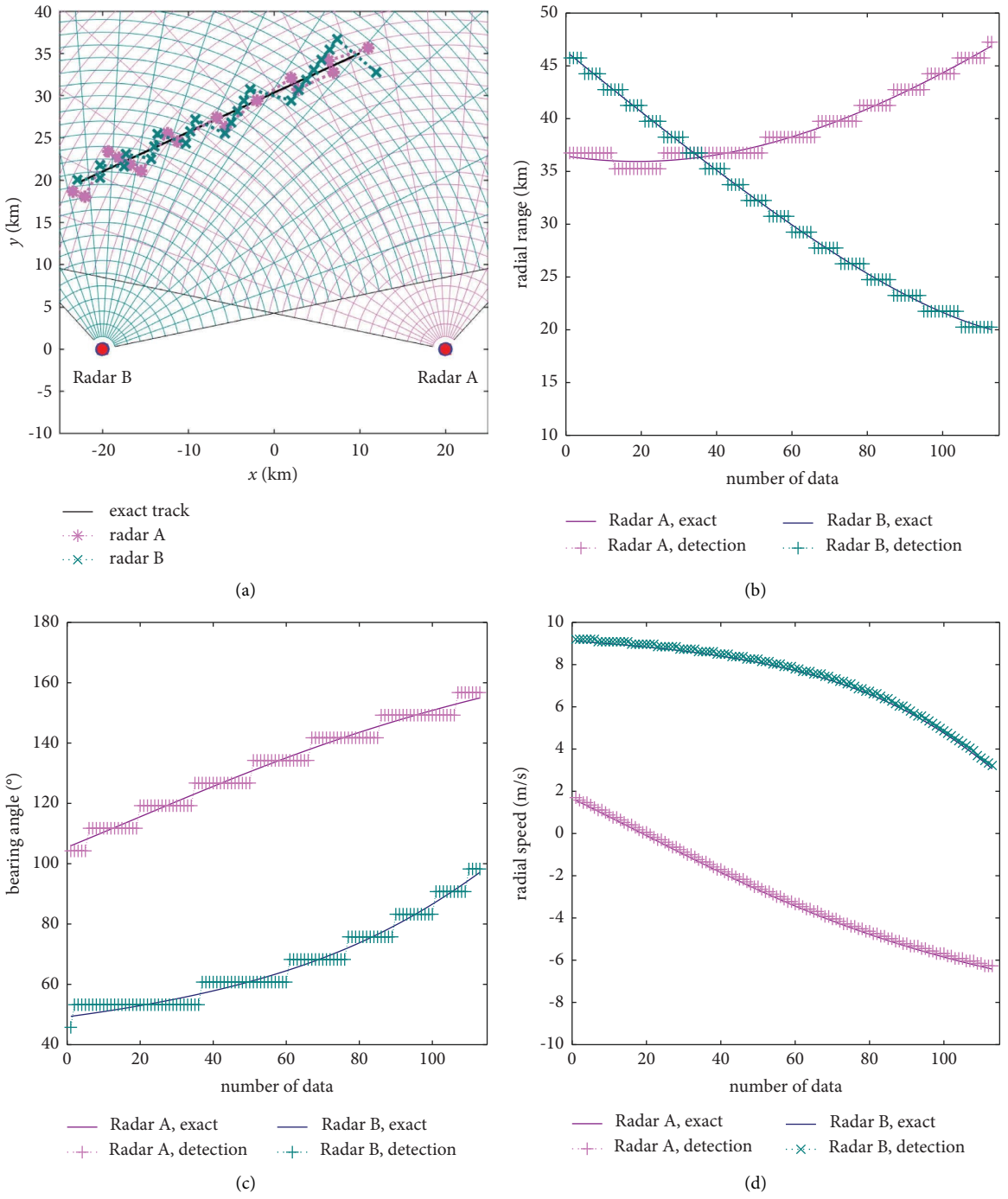

Figure 6: Effect of low spatial and temporal resolution on the radar measurement in two HFSWR stations: (a) measured track, (b) radial range, (c) bearing, and (d) radial speed.

Table 4: RMSE of radial distance, bearing angle, and speed on the detection of HFSWR.

Parameters of measurement	RMSE	
	Radar A	Radar B
Radial range (km)	0.499	0.426
Bearing angle (°)	2.231	2.202
Radial speed (m/s)	0.121	0.120

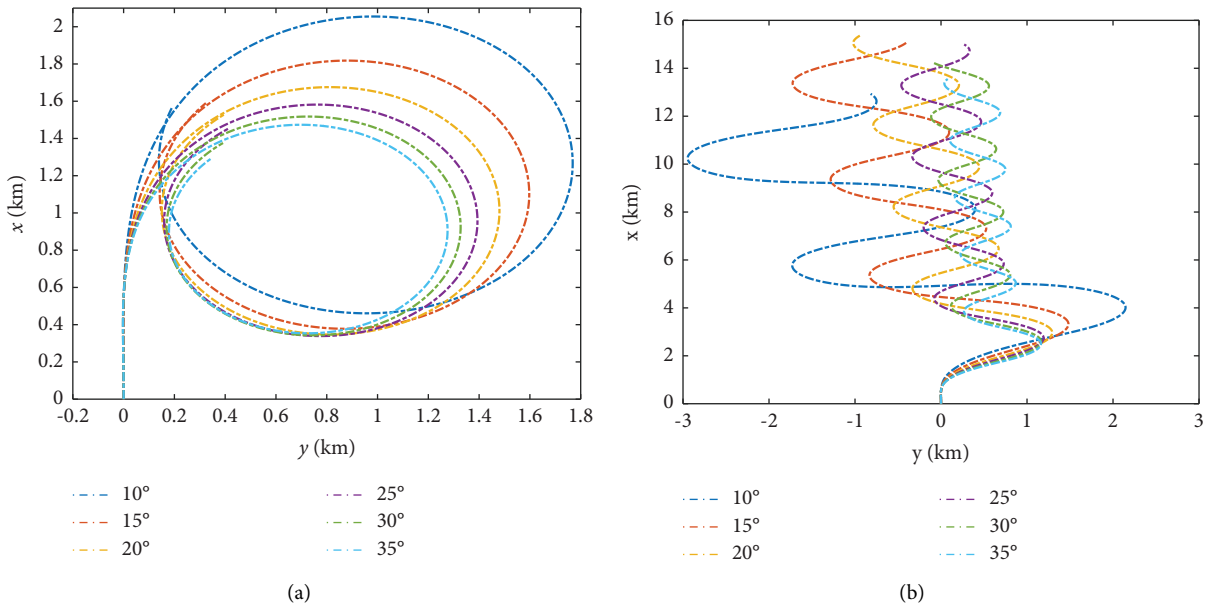

Figure 7: The ship maneuvers generated by MANSIM: (a) turning and (b) zigzag.

Figure 7(b) depicts the results of the zigzag maneuver with various maximum rudder angles. The higher steering angle gives a narrower transverse variation. Since the MMG model considers many hydrodynamics aspects during its movement, it provides a more realistic ship maneuver than the result of general shape equations.

Next, the position and heading of each ship track were randomized by the Monte Carlo simulation to observe the effect of spatial resolution variation statistically. Figure 8 visualizes the randomized linear tracks generated by the MC simulation.

3.3. Test on Linear Ship Motions. Initially, all-considered tracking algorithms were tested on 100 randomly positioned linear tracks on the radar scene. The RMSEs of tracking results are shown in Figure 9, which quantizes that all trackers can obtain the RMSE about the radar resolution. Note that the radar range resolution is 1.5 km, as listed in Table 1. However, the range error is increased in the patch far from the radar station due to the higher azimuth error. After comparing the result of the tracking error with and without the tracking algorithm, it can be concluded that the tracker can improve radar detection.

Table 4 shows both trackers' RMSE of distance, confirming that the EKF tracker performs better on the linear track while the KF tracker has an error close to the measurement error. The effect of low radar resolution causes the random detection error, as shown in Figure 6(a). Since the error is sometimes higher than the ship movement in the sampling period, the error can significantly decrease the tracking performance of all algorithms. However, the EKF suffers the lower effect due to its flexibility in the error model.

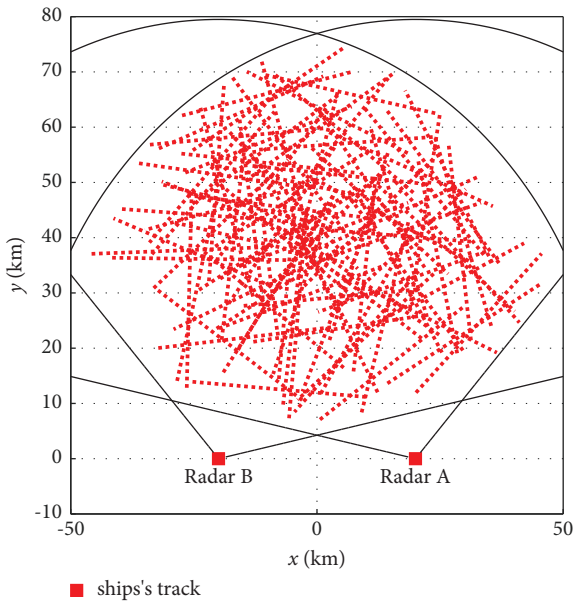

Figure 8: Result of Monte Carlo simulation to randomize the initial position and heading for the linear tracks.

3.4. Test on Turning Maneuvers. Secondly, the trackers were employed on the mixed linear and turning tracks. The test results are shown in Figure 10 for various turning angles. The results show that adding 20 minutes of turning is drastically decreased all tracker's performance.

The UKF has the lowest error in the turning track, while the EKF is slightly higher than UKF. The linearization method of UKF is naturally more stable to track in a higher nonlinear system. The PF obtains the most error. The tracks are spread out to occupy all radar coverage areas by the Monte Carlo simulation in the track generation. On the

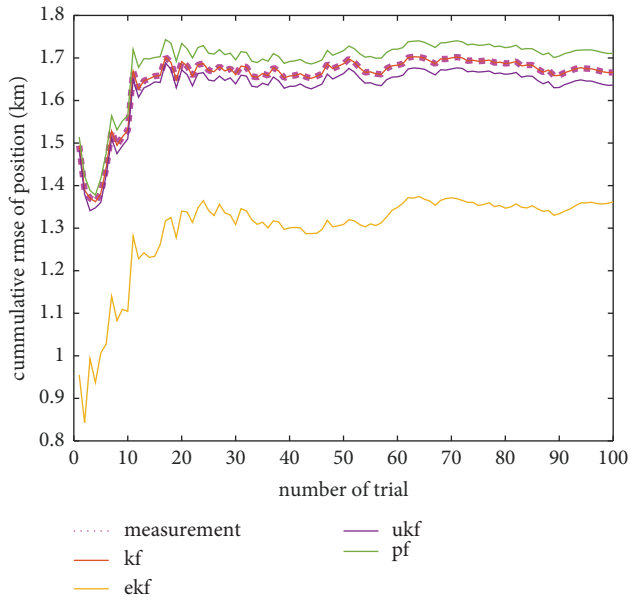

Figure 9: Results of tracking process in linear ship motions by the tested trackers on radar A.

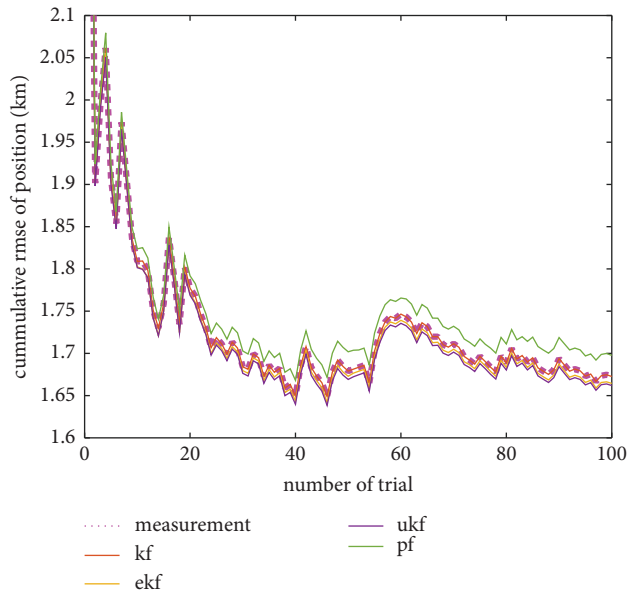

Figure 10: Results of tracking process in the turning maneuvers by the tested trackers.

other hand, the PF algorithm generates the particle and gives the weight factor to the most repeated point.

3.5. Test on Zigzag Maneuvers. The last assessment was tracking the zigzag maneuvers. The results are depicted in Figure 11. In this scenario, the zigzag plot is in the entire duration. Similar to the test on turning angle, the UKF is superior to other methods. It underlines the ability of the UKF tracker to recognize any changes in target motions.

3.6. Comparison of Tracking Algorithms. It has been presented in the prior discussion that the ship detection and tracking process on the HFSWR is challenging due to its low spatial and temporal resolutions. The tracking process becomes highly sophisticated when the target moves with high maneuvers. Therefore, it is crucial to test the tracking algorithm's performance on the maneuvering target.

Table 5 and Figure 12 summarize the tracking errors of considered trackers to work on the radar with an 80 km maximum range, 1.5 km range resolution, and 32 s time resolution. The results in Table 4 show that all trackers can work well on linear ship tracks with RMSE of about 1.3 to 1.8 km. The testing tracks consist of linear and maneuvering ship motions. The tracking performance on the linear track shows that the EKF performs the best among other algorithms. The indicator parameters calculation is 1.368 km, 0.526 km, 1.550°, and 0.005 m/s for the absolute position,

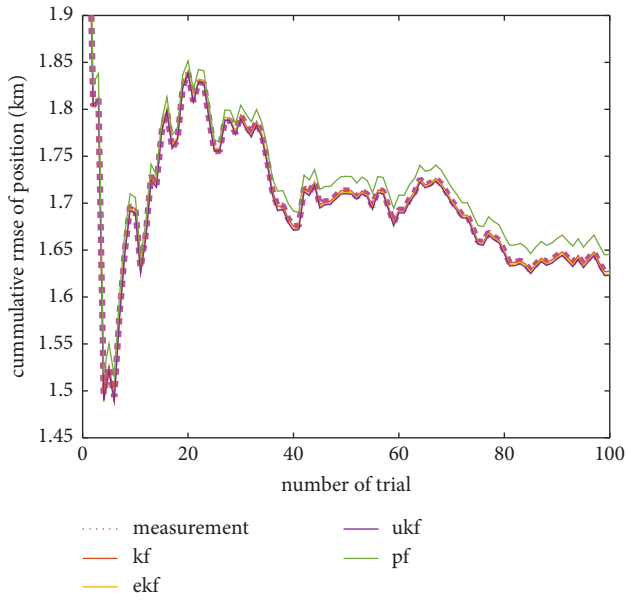

Figure 11: Results of the tracking process in the zigzag maneuvers by the tested trackers.

Table 5: The performance indicator of the ship tracking algorithm.

Performance indicators	Tracking algorithm	Radar A			Radar B			Average	
		Linear	Turning	Zigzag	Linear	Turning	Zigzag	Linear	Maneuvers
RMSE of position (km)	KF	1.666	1.673	1.627	1.696	1.620	1.702	1.681	1.655
	EKF	**1.362**	1.665	1.624	**1.374**	1.616	1.699	**1.368**	1.651
	UKF	1.636	**1.662**	**1.623**	1.667	**1.613**	**1.698**	1.652	**1.649**
	PF	1.711	1.698	1.645	1.737	1.650	1.722	1.724	1.678
RMSE of radial range (km)	KF	0.655	0.646	0.636	0.649	0.645	0.642	0.652	0.642
	EKF	**0.523**	0.639	**0.634**	**0.523**	**0.639**	**0.640**	**0.526**	**0.638**
	UKF	0.632	**0.639**	0.635	0.626	0.640	0.642	0.629	0.639
	PF	0.632	0.669	1.654	0.626	0.661	0.655	0.629	0.660
RMSE of bearing angle (°)	KF	1.891	1.918	1.851	1.938	1.880	2.039	1.914	1.922
	EKF	**1.542**	1.916	1.850	**1.556**	1.884	2.038	**1.550**	1.922
	UKF	1.883	**1.912**	**1.848**	1.929	**1.879**	**2.035**	1.906	**1.919**
	PF	1.895	1.947	1.861	1.937	1.922	2.053	1.916	1.944
RMSE of speed (m/s)	KF	0.356	0.394	0.354	0.374	0.413	0.357	0.375	0.380
	EKF	**0.004**	0.177	0.153	**0.005**	0.177	0.153	**0.005**	0.165
	UKF	0.011	**0.177**	**0.153**	0.011	**0.177**	**0.153**	0.011	**0.165**
	PF	0.013	0.182	0.157	0.013	0.182	0.57	0.013	0.170

The minimum error in each case is signed in bold front.

radial range, bearing angle, and speed. The results of tracking the maneuvering target ship showed that UKF achieved the lowest error indicators, but it just slightly differs from the EKF. The RMSE of absolute position, radial range, bearing angle, and speed is 1.649 km, 0.639 km, 1.919°, and 0.165 m/s, respectively.

Finally, it is worth noticing that the MMG model can generate free-running maneuvers with many different types of vessels as long as the required parameters are known. Accordingly, it is possible to evaluate the tracking performance with any plot by following the proposed procedures in this work.

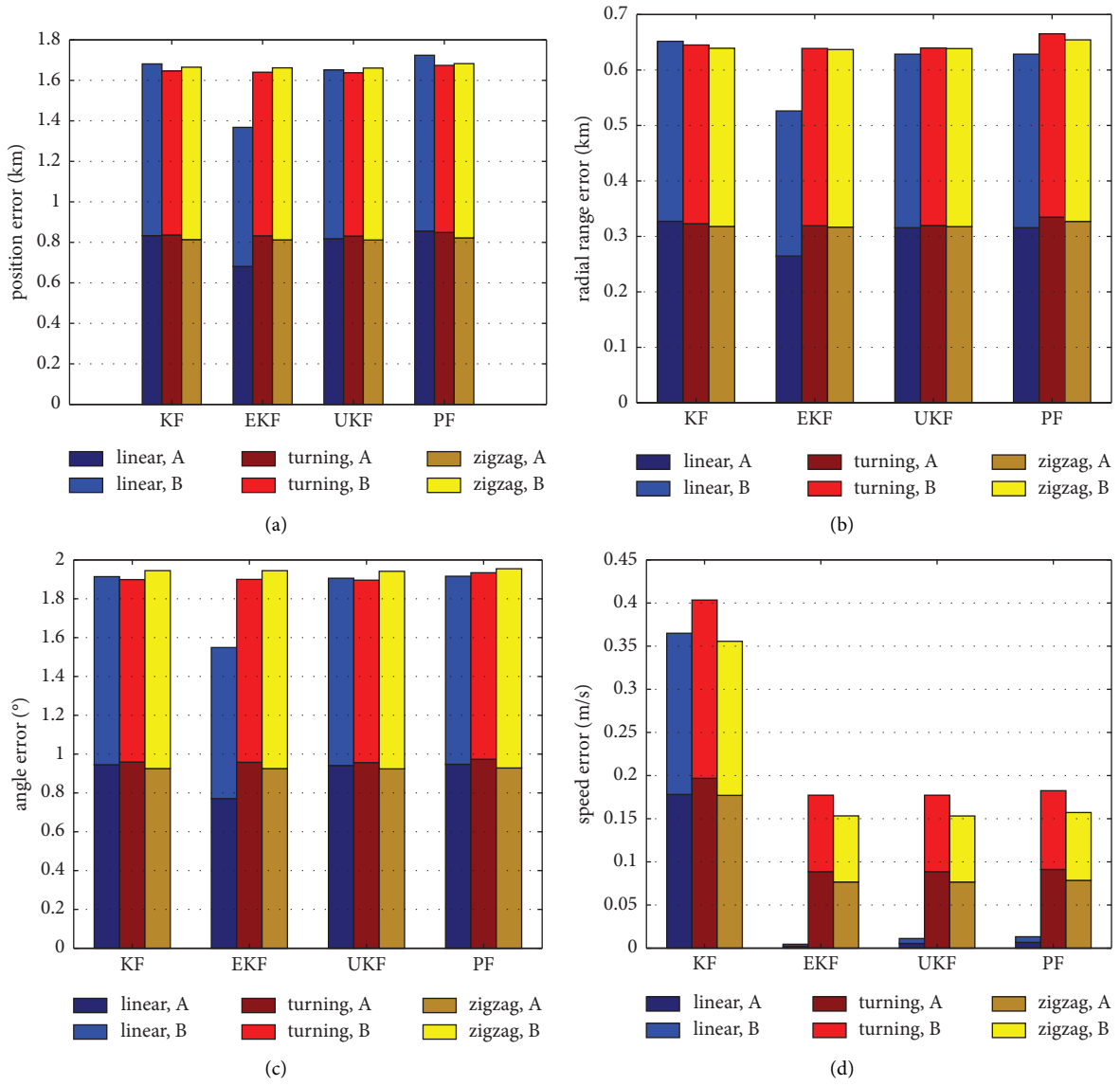

FIGURE 12: The comparison of tracking performance measured by the indicator parameters: (a) absolute position, (b) radial range, (c) bearing angle, and (d) absolute speed.

4. Conclusions

The paper presents the procedures to evaluate the tracking algorithm performance in HFSWR in any possible ship maneuver by utilizing the MMG model. The target motion generated by the proposed model can be inputted into the radar simulator to get successive target detection on which the tracking algorithms are applied. This proposed method allows the tracker to test realistic ship maneuvers which are not provided by existing mathematical models or AIS empirical records.

The proposed evaluation mechanism is implemented to assess the performance of KF, EKF, UKF, and PF filters to trail three maneuvers: linear, turning, and zigzag. The ship detections are conducted on the radar simulator with an 80 km maximum range and 1.5 km range resolution. The tracking performance is analyzed by calculating the RMSE of four parameters, i.e., absolute position, radial range, bearing angle, and speed. The evaluation results show that the EKF tracker has the slightest error for the linear track with RMSE of absolute position, radial range, bearing angle, and speed are 1.368 km, 0.526 km, 1.550°, and 0.005 m/s, respectively. Otherwise, the UKF performs slightly better than EKF for the high maneuver targets. The RMSEs of absolute position, radial range, bearing angle, and speed are 1.649 km, 0.639 km, 1.919°, and 0.165 m/s, respectively. The assessment results agree with the findings of other works.

The current work evaluates four basic tracking algorithms for a method trial. The work has been accomplished to develop the HF radar simulator, which is interconnected to the MMG model to include the ship maneuver in the radar simulation. The simulator has also been incorporated to assess the ship tracking performance in the HF radar. Based on the current achievement, the simulator can be

enhanced to evaluate more tracking algorithms and variations of ship maneuvers. They are reminded of future works.

Data Availability

The data used to support the findings of this study are available from the corresponding author upon request.

Conflicts of Interest

The authors declare that there are no conflicts of interest regarding the publication of this paper.

Acknowledgments

The authors would like to thank the Minister of Higher Education for supporting this research through the Hibah Penelitian Disertasi Doktor Research Grant with Contract no. 2309/UN1/DITLIT/DIT-LIT/PT/2021.

References

[1] D. Nikolic, "Maritime over the horizon sensor integration: HFSWR data fusion algorithm," *Remote Sensing*, vol. 11, no. 7, p. 852, 2019.

[2] Y. M. Wang, X. P. Mao, J. Zhang, and Y. G. Ji, "Ship target detection in sea clutter of hfswr based on spatial blind filtering," *IET Conference Publications*, vol. 2015, p. CP677, 2015.

[3] S. Shang, K. He, Z. Wang, and X. Yang, "Stationary time statistical property of ionospheric clutter in high-frequency surface-wave radar," *Journal of Electrical and Computer Engineering*, Article ID 2450191, 6 pages, 2019.

[4] S. Maresca, P. Braca, and J. Horstmann, "Data fusion performance of HFSWR Systems for ship traffic monitoring," in *Proceedings of the 16th International Conference on Information Fusion*, pp. 1273–1280, Istanbul, Turkey, July 2013.

[5] W. Jiabao, Y. Guochen, G. Liqing, L. Yongxin, and N. Xiaomin, "HFSWR ship trajectory tracking and fusion with AIS using Kalman filter," in *Proceedings of the 29th Chinese Control and Decision Conference*, pp. 456–461, Chongqing, China, May 2017.

[6] Y. J. Chung, L. Z. H. Chuang, and W. C. Yang, "Feasibility studies of ship detections using seasonde HF radar," in *Proceedings of the 2013 IEEE International Geoscience and Remote Sensing Symposium - IGARSS*, pp. 2892–2895, Melbourne, Australia, July 2013.

[7] W. Sun, Z. Pang, W. Huang, Y. Ji, and Y. Dai, "Vessel velocity estimation and tracking from Doppler echoes of T/R-R composite compact HFSWR," *Ieee Journal of Selected Topics in Applied Earth Observations and Remote Sensing*, vol. 14, pp. 4427–4440, 2021.

[8] K. Jaskolski, L. Marchel, A. Felski, M. Jaskolski, and M. Specht, "Automatic identification system (AIS) dynamic data integrity monitoring and trajectory tracking based on the simultaneous localization and mapping (SLAM) process mode," *Sensors*, vol. 21, pp. 1–19, 2021.

[9] K. Wang, P. Zhang, J. Niu, W. Sun, L. Zhao, and Y. Ji, "A performance evaluation scheme for multiple object tracking with HFSWR," *Sensors*, vol. 19, no. 6, pp. 1–20, 2019.

[10] W. Sun, M. Ji, W. Huang, Y. Ji, and Y. Dai, "Vessel tracking using bistatic compact HFSWR," *Remote Sensing*, vol. 12, no. 8, pp. 1266–1268, 2020.

[11] L. Zhang, Y. Jiang, Y. Li, G. Li, and Y. Ji, "Adaptive maneuvering target tracking with 2-HFSWR multisensor surveillance system," *IEEE Aerospace and Electronic Systems Magazine*, vol. 32, no. 12, pp. 70–76, 2017.

[12] S. Abdel-Latif, M. Abdel-Geliel, and E. Eldin Zakzouk, "Simulation of ship maneuvering behavior based on the modular mathematical model," in *Proceedings of the 2013 21st Mediterranean Conference on Control and Automation, MED 2013 - Conference*, pp. 94–99, Chania, Crete, Greece, June 2013.

[13] H. Yasukawa and Y. Yoshimura, "Introduction of MMG standard method for ship maneuvering predictions," *Journal of Marine Science and Technology*, vol. 20, no. 1, pp. 37–52, 2015.

[14] Mansim, "MANSIM V2.01," 2021, https://www.mansim.org/.

[15] O. F. Sukas, O. K. Kinaci, and S. Bal, "Theoretical background and application of MANSIM for ship maneuvering simulations," *Ocean Engineering*, vol. 192, Article ID 106239, 2019.

[16] R. H. Iswandi and S. B. Wibowo, "Simulation of signal processing for ship detection on two overlapping HF radars with FMCW waveforms," in *Proceedings of the 12th International Conference on Information Technology and Electrical Engineering*, pp. 39–44, Yogyakarta, Indonesia, October 2020.

[17] E. A. Dzvonkovskaya, K. Gurgel, H. Rohling, and T. Schlick, "HF radar WERA application for ship detection and tracking," *European Journal of Navigation*, vol. 3, no. 3, pp. 18–25, 2009.

[18] C. Balanis, *Antenna Theory: Analysis and Design*, John Wiley & Sons, Hoboken, NJ, USA, 3rd edition, 2005.

[19] D. Nikolio, Z. Popovic, M. Borenovio et al., "Multi-radar multi-target tracking algorithm for maritime surveillance at OTH distances," in *Proceedings of the 2016 17th International Radar Symposium (IRS)*, Krakow, Poland, May 2016.

[20] K. E. Laws, J. F. Vesecky, M. N. Lovellette, and J. D. Paduan, "Ship tracking by HF radar in coastal waters," in *Proceedings of the OCEANS 2016 MTS/IEEE Monterey*, Monterey, CA, USA, September 2016.

[21] W. Sun, W. Huang, Y. Ji et al., "A vessel azimuth and course joint Re-estimation method for compact HFSWR," *IEEE Transactions on Geoscience and Remote Sensing*, vol. 58, no. 2, pp. 1041–1051, 2020.

[22] F. Mo, X. Wu, X. Yue, and L. Zhang, "Research on maritime target tracking for high frequency over-the-horizon radar," in *Proceedings of the 2020 IEEE International Conference on Computational Electromagnetics (ICCEM)*, pp. 119-120, Singapore, August 2020.

[23] N. Stojkovic, "An implementation of tracking algorithm for over-the-horizon surface wave radar," in *Proceedings of the 24th Telecommunications Forum*, pp. 24–27, Belgrade, Serbia, November 2016.

[24] B. Balaji and Z. Ding, "A performance comparison of nonlinear filtering techniques based on recorded radar datasets," *SPIE Proceedings*, vol. 7445, p. 74450Q, 2009.

[25] G. Vivone, P. Braca, and J. Horstmann, "Knowledge-based multitarget ship tracking for HF surface wave radar systems," *IEEE Transactions on Geoscience and Remote Sensing*, vol. 53, no. 7, pp. 3931–3949, 2015.

[26] S. Konatowski, P. Kaniewski, and J. Matuszewski, "Comparison of estimation accuracy of EKF, UKF and PF filters," *Annual of Navigation*, vol. 23, no. 1, pp. 69–87, 2016.

[27] J. Yang, X. Liu, B. Yang, J. Lu, and G. Liao, "Detection and speed estimation of moving target based on phase compensation and coherent accumulation using fractional fourier transform," *Sensors*, vol. 20, no. 5, p. 1410, 2020.